

# Viscosity of hadron matter within relativistic mean-field based model with scaled hadron masses and couplings

A.S. Khvorostukhin,<sup>1,\*</sup> V.D. Toneev,<sup>2,†</sup> and D.N. Voskresensky<sup>2,‡</sup>

<sup>1</sup>*Institute of Applied Physics, Moldova Academy of Science, Kishineu, Moldova*

<sup>2</sup>*Gesellschaft für Schwerionenforschung mbH, Darmstadt, Germany*

The shear ( $\eta$ ) and bulk ( $\zeta$ ) viscosities are calculated in a quasiparticle relaxation time approximation for a hadron matter described within the relativistic mean-field based model with scaled hadron masses and couplings. Comparison with results of other models is presented. We demonstrate that a small value of the shear viscosity to entropy density ratio required for explaining a large elliptic flow observed at RHIC may be reached in the hadron phase. Relatively large values of the bulk viscosity are noted in the case of a baryon enriched matter.

PACS: 24.10.Nz, 25.75.-q

## I. INTRODUCTION

In the past, transport coefficients for the nuclear matter were studied in [1, 2, 3, 4]. Recently, the interest in the transport coefficient issue has sharply been increased in heavy-ion collision physics, see review-article [5]. Values of the elliptic flow  $v_2$  observed at RHIC [6] proved to be larger than at SPS. This finding is interpreted as that a quark-gluon plasma (QGP) created at RHIC behaves as a nearly perfect fluid with a small value of the shear viscosity-to-entropy density ratio,  $\eta/s$ . The latter statement was confirmed by non-ideal hydrodynamic analysis of these data [7]. Thereby, it was claimed [8, 9, 10] that a new state produced at high temperatures is most likely not a weakly interacting QGP, as it was originally assumed, but a strongly interacting QGP. The interest was also supported by a new theoretical perspective, namely,  $\mathcal{N} = 4$  supersymmetric Yang-Mills gauge theory using the

---

\*hvorost@theor.jinr.ru; Joint Institute for Nuclear Research, Dubna, Russia

†toneev@theor.jinr.ru; Joint Institute for Nuclear Research, Dubna, Russia

‡voskre@pisem.net; Moscow Engineering Physical Institute, Moscow, Russia

Anti de-Sitter space/Conformal Field Theory (AdS/CFT) duality conjecture. Calculations in this strongly coupled theory demonstrate that there is minimum in the  $\eta/s$  ratio [11]:  $\eta/s \approx 1/(4\pi)$ . It was thereby conjectured that this relation is in fact a lower bound for the specific shear viscosity in all systems [5] and that the minimum is reached in the hadron-quark transition critical point (at  $T = T_c$ ).

In this paper, we continue investigation of the shear and bulk viscosities performed in Ref. [12] within the quasiparticle model in the relaxation time approximation. We describe the hadron phase ( $T < T_c$ ) in terms of the quasiparticle relativistic mean-field-based model with the scaling hadron masses and couplings (SHMC) been successfully applied to the description of heavy ion collision reactions [13, 14], see sect.2. Then in sect.3 we calculate the shear and bulk viscosities and compare our results with results of previous works. In sect. 4 we formulate our conclusions.

## II. DESCRIPTION OF HADRON MATTER IN THE SHMC MODEL

### A. Formulation of the model

Within our relativistic mean-field SHMC model [13, 14] we present the Lagrangian density of the hadronic matter as a sum of several terms:

$$\mathcal{L} = \mathcal{L}_{\text{bar}} + \mathcal{L}_{\text{MF}} + \mathcal{L}_{\text{ex}} . \quad (1)$$

The Lagrangian density of the baryon component interacting via  $\sigma, \omega$  mean fields is as follows:

$$\mathcal{L}_{\text{bar}} = \sum_{b \in \{\text{bar}\}} \left[ i \bar{\Psi}_b \left( \partial_\mu + i g_{\omega b} \chi_\omega \omega_\mu \right) \gamma^\mu \Psi_b - m_b^* \bar{\Psi}_b \Psi_b \right] . \quad (2)$$

The considered baryon set is  $\{b\} = N(938), \Delta(1232), \Lambda(1116), \Sigma(1193), \Xi(1318), \Sigma^*(1385), \Xi^*(1530),$  and  $\Omega(1672)$ , including antiparticles. The used  $\sigma$ -field dependent effective masses of baryons are [13, 14, 15]

$$m_b^*/m_b = \Phi_b(\chi_\sigma \sigma) = 1 - g_{\sigma b} \chi_\sigma \sigma / m_b , \quad b \in \{b\} . \quad (3)$$

In Eqs. (2), (3)  $g_{\sigma b}$  and  $g_{\omega b}$  are coupling constants and  $\chi_\sigma(\sigma)$ ,  $\chi_\omega(\sigma)$  are coupling scaling functions.

The  $\sigma$ -,  $\omega$ -meson mean field contribution is given by

$$\begin{aligned}\mathcal{L}_{\text{MF}} &= \frac{\partial^\mu \sigma \partial_\mu \sigma}{2} - \frac{m_\sigma^{*2} \sigma^2}{2} - U(\chi_\sigma \sigma) - \frac{\omega_{\mu\nu} \omega^{\mu\nu}}{4} + \frac{m_\omega^{*2} \omega_\mu \omega^\mu}{2}, \\ \omega_{\mu\nu} &= \partial_\mu \omega_\nu - \partial_\nu \omega_\mu, \quad U(\chi_\sigma \sigma) = m_N^4 \left( \frac{b}{3} f^3 + \frac{c}{4} f^4 \right), \quad f = g_{\sigma N} \chi_\sigma \sigma / m_N.\end{aligned}\tag{4}$$

There exist only  $\sigma$  and  $\omega_0$  mean field solutions of equations of motion. The mass terms of the mean fields are

$$m_m^*/m_m = |\Phi_m(\chi_\sigma \sigma)|, \quad \{m\} = \sigma, \omega.\tag{5}$$

The dimensionless scaling functions  $\Phi_b$  and  $\Phi_m$ , as well as the coupling scaling functions  $\chi_m$ , depend on the scalar field in combination  $\chi_\sigma(\sigma) \sigma$ . Following [15] we assume approximate validity of the Brown-Rho scaling ansatz in the simplest form

$$\Phi = \Phi_N = \Phi_\sigma = \Phi_\omega = \Phi_\rho = 1 - f.\tag{6}$$

The third term in the Lagrangian density (1) includes meson quasiparticle excitations:  $\pi; K, \bar{K}; \eta(547); \sigma', \omega', \rho'; K^{*\pm,0}(892), \eta'(958), \phi(1020)$ . The choice of parameters and other details of the SHMC model can be found in [13, 14].

## B. Thermodynamical quantities

Within SHMC model we calculate different thermodynamical quantities in thermal equilibrium hadron matter at fixed temperature  $T$  and baryon chemical potential  $\mu_{\text{bar}}$ . In Fig. 1 (left panel) we show the square of the sound velocity  $c_s^2 = dP/d\varepsilon$  ( $P$  is pressure,  $\varepsilon$  is energy density), as function of temperature at zero baryon chemical potential,  $\mu_{\text{bar}} = 0$ , for the SHMC model (solid line) and compare this result with that for the ideal gas (IG) model with the same hadron set as in the SHMC model (long-dashed line), for the  $\pi + \rho$  mixture (dash-double dot) and for purely pion system (dash-dotted). As is seen from this figure, for the purely pion IG the  $c_s^2$  monotonously increases with increase of the temperature approaching the ultrarelativistic limit  $c_s^2 = 1/3$  at high temperatures. For the pion-rho meson mixture, the  $c_s^2$  exhibits a shallow minimum at  $T \sim 170$  MeV. The minimum (in the same temperature region) becomes more pronounced for multi-component systems (see dash curve). At  $T \lesssim 50$  MeV the pion contribution is a dominant one, thereby all curves

coincide<sup>1</sup>. The curves for the SHMC model and the IG model calculated with the same hadron set coincide for  $T \lesssim 100$  MeV. At  $T > 50$  MeV heavier mesons start to contribute that slows down the growth of pressure and then results in significant decrease of  $c_s^2$ , contrary to the case of the one-component pion gas. Within the SHMC model  $c_s^2$  gets pronounced minimum at  $T \simeq 180$  MeV caused by a sharp decrease of the in-medium hadron masses at these temperatures (see the right panel in Fig. 1, where effective masses of the nucleon,  $\omega$ ,  $\rho$  and  $\sigma$  excitations are presented). The minimum of the sound velocity (at  $T = T_c \simeq 180$  MeV) can be associated with a kind of phase transition, e.g. with the hadron-QGP cross-over, as it follows from the detailed analysis of the lattice data, see [16].

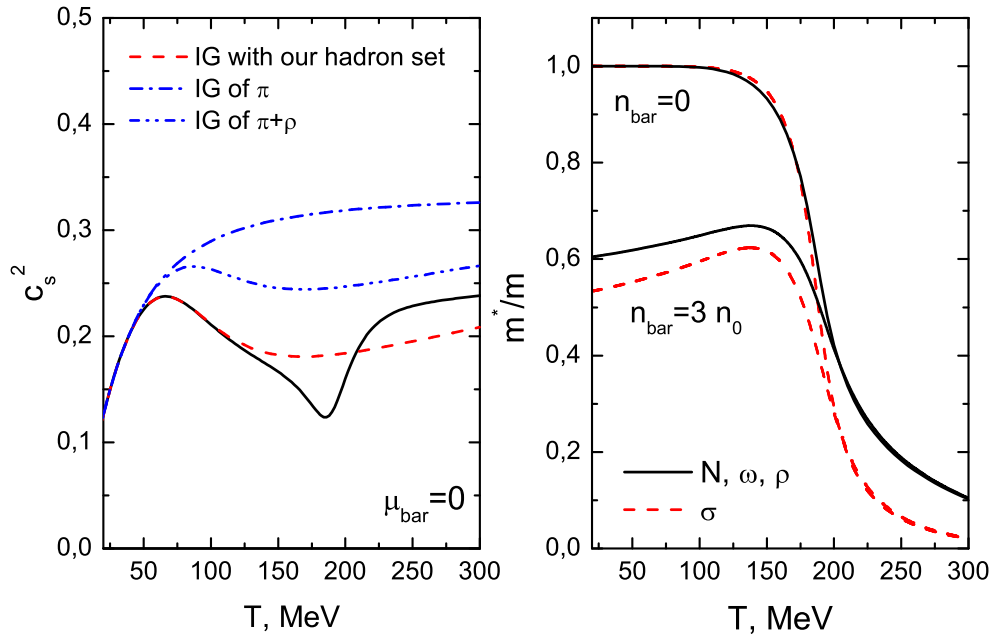


Рис. 1: Left panel: The sound velocity squared in hadron matter as function of the temperature at zero baryon chemical potential. Solid line – calculation within the SHMC model. Other notations are given in the legend. Right panel: The temperature dependence of effective masses of the nucleon,  $\omega$  and  $\rho$  excitations (solid line) and of the  $\sigma$ -meson excitation (dashed line) calculated within the SHMC model for two values of the baryon density.

Note that in the Hagedorn-gas model [17] (for the Hagedorn mass  $m \rightarrow \infty$ ) one gets  $c_s^2 \rightarrow 0$  at  $T = T_c$ , whereas in the mass-truncated Hagedorn-gas model the behavior very close to that we have in case of the IG model is observed.

<sup>1</sup> Note that within the SHMC model pions are treated as an ideal gas of free particles

In Fig. 2 we present the lattice data for the reduced energy density and the pressure together with our SHMC model results. Following [14] we use suppressed coupling constants  $g_{\sigma b}$  (except for nucleons). This guarantees that even above  $T_c$  up to the temperature  $T \sim 220$  MeV the EoS computed in the SHMC model is in agreement with the lattice data for the

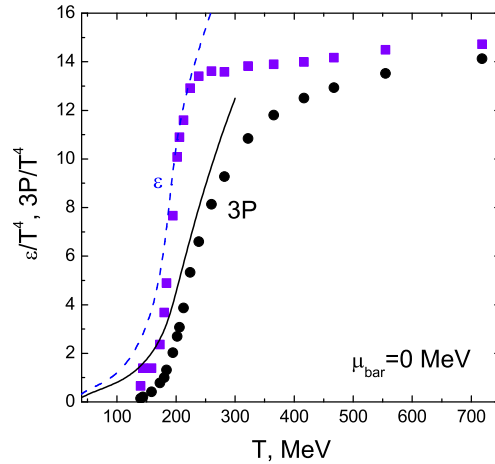


Рис. 2: The reduced triple pressure and the energy density at  $\mu_{\text{bar}} = 0$ . Points are QCD lattice result [16]. The hadronic SHMC results are plotted by solid and dash lines, respectively.

pressure and energy density. At higher temperatures the SHMC model requires additional modifications, although in reality the quark-gluon degrees of freedom should be taken into account already for  $T > T_c \sim 180$  MeV.

### III. SHEAR AND BULK VISCOSITIES OF THE SHMC MODEL

#### A. Collisional viscosity, derivation of equations

Sasaki and Redlich [12] derived expressions for the shear and bulk viscosities in the case when the quasiparticle spectrum is given by  $E(\vec{p}) = \sqrt{\vec{p}^2 + m^{*2}(T, \mu)}$ . We perform a similar derivation, but in the presence of mean fields. In the latter case one should additionally take into account that quasiparticle distributions depend on the mean fields.

In order to calculate viscosity coefficients one needs an expression for spatial components of the energy momentum tensor corresponding to the Lagrangian density (1):

$$T^{ij} = T_{\text{MF}}^{ij} + \sum_{b \in \{\text{bar}\}} T_b^{ij} + \sum_{\text{bos} \in \{\text{ex}\}} T_{\text{bos}}^{ij}, \quad (7)$$

where  $i, j = 1, 2, 3$  and the mean-field contribution is as follows

$$T_{\text{MF}}^{ij} = \partial^i \sigma \partial^j \sigma - \partial^i \omega_0 \partial^j \omega_0 + \left( \frac{1}{2} [\partial^i \sigma \partial^j \sigma - \partial^i \omega_0 \partial^j \omega_0 + m_\sigma^{*2} \sigma^2 - m_\omega^{*2} \omega_0^2] + U(\sigma) \right) g^{ij} \quad (8)$$

with  $m_\sigma^*$  and  $m_\omega^*$  given by Eq. (5).

The quasiparticle (fermion and boson excitation) contribution is given by

$$T_a^{ij} = \int d\Gamma \frac{p_a^i p_a^j}{E_a} F_a, \quad a \in (\text{bos.}, \text{bar}), \quad E_a = \sqrt{\vec{p}^2 + m^{*2}}, \quad \Gamma = \nu_a \frac{d^3 p_a}{(2\pi)^3}, \quad (9)$$

where  $\nu_a$  is the degeneracy factor.

The quasiparticle distribution function  $F_b$  for baryon components in the presence of mean fields fulfills the Boltzmann kinetic equation [18],

$$\left( p_b^\mu \partial_\mu - g_{\omega b} p_\mu \omega^{\mu\nu} \frac{\partial}{\partial p_b^\nu} + m_b^* \partial^\nu m_b^* \frac{\partial}{\partial p_b^\nu} \right) \tilde{F}_b = St \tilde{F}_b; \quad (10)$$

with  $\tilde{F}_b(p_b, x_b) = \delta(p_b^2 - m_b^{*2}) F_b(\vec{p}_b, x_b)$ .

The local equilibrium boson or baryon distribution is given as follows:

$$F_a^{\text{loc.eq.}}(\vec{p}_a, x_a) = \left[ e^{(E_a - \vec{p}_a \vec{u} - \mu_a + t_a^{\text{vec}} X_a^0)/T} \pm 1 \right]^{-1}, \quad X_a^0 = g_{\omega a} \chi_\omega \omega_0, \quad (11)$$

where we suppressed  $\vec{u}^2$  terms for  $|\vec{u}| \ll 1$ . Here the upper sign (+) is for fermions and (−) is for bosons, and the vector particle charge is  $t_a^{\text{vec}} = \pm 1$  or 0;  $g_{\omega a} \neq 0$  only for  $a \in \text{bar}$  in our model. Considering only slightly inhomogeneous solutions and using  $|\vec{u}| \ll 1$  we may drop the terms  $\propto \vec{u}^2$  and  $\propto \vec{u} \nabla \omega_0$  in the kinetic equation (10). Then kinetic equations for boson and baryon components acquire ordinary quasiparticle form

$$\frac{\partial F_a}{\partial t} + \frac{\partial E_a}{\partial \vec{p}_a} \frac{\partial F_a}{\partial \vec{r}_a} - \frac{\partial E_a}{\partial \vec{r}_a} \frac{\partial F_a}{\partial \vec{p}_a} = \frac{p_a^\mu}{E_a} \frac{\partial F_a}{\partial x_a^\mu} = St F_a, \quad (12)$$

where  $p_a^\mu = (E_a(\vec{p}_a, \vec{r}_a, \sigma, \omega), \vec{p}_a)$ . We used that  $\partial E_a / \partial \vec{p}_a = \vec{p}_a / E_a$ . Since calculating the viscosity, we need only terms with velocity gradients, we further put  $\partial E_a / \partial \vec{r}_a = (\partial E_a / \partial \mu_a) \vec{\nabla}_a \mu_a + (\partial E_a / \partial T) \vec{\nabla}_a T = 0$ .

In the relaxation time approximation

$$St F_a = -\delta F_a / \tau_a, \quad \delta F_a = F_a - F_a^{\text{loc.eq.}}. \quad (13)$$

Here  $\tau_a$  denotes the relaxation time of the given species. Generally, it depends on the quasiparticle momentum  $\vec{p}_a$  and the quasiparticle energy  $E_a(\vec{p}_a)$ .

The averaged partial relaxation time  $\tilde{\tau}_a$  is related to the cross section as

$$\tilde{\tau}_a^{-1}(T, \mu) = \sum_{a'} n_{a'}(T, \mu) \langle v_{aa'} \sigma_{aa'}^t(v_{aa'}) \rangle, \quad (14)$$

where  $n_{a'}$  is the density of  $a'$ -species,  $\sigma_{aa'}^t = \int d\cos\theta \, d\sigma(aa' \rightarrow aa')/d\cos\theta (1 - \cos\theta)$  is the transport cross section, in general, accounting for in-medium effects and  $v_{aa'}$  is the relative velocity of two colliding particles  $a$  and  $a'$  in case of binary collisions. Angular brackets denote a quantum mechanical statistical average over an equilibrated system. In reality, the cross sections entering the collision integral and the corresponding relaxation time  $\tau_a$  in (13) may essentially depend on the particle momentum. Thus, averaged values  $\tilde{\tau}_a^{-1}$  given by Eq. (14) yield only a rough estimate for the values  $\tau_a^{-1}$  which we actually need for calculation of viscosity coefficients, see below Eqs. (21) and (22).

In the relaxation time approximation from Eqs. (12), (13) we obtain

$$\delta F_a = -\frac{\tau_a}{E_a} p_a^\mu \frac{\partial F_a^{\text{loc.eq.}}}{\partial x_a^\mu}, \quad (15)$$

and then the variation of the energy-momentum tensor (7) becomes:

$$\delta T^{ij} = -\sum_a \int d\Gamma \left\{ \tau_a \frac{p_a^i p_a^j}{E_a^2} p_a^\mu \partial_\mu F_a \right\}_{\text{loc.eq.}} + \delta\sigma \left\{ \frac{\partial T^{ij}}{\partial\sigma} \right\}_{\text{loc.eq.}} + \delta\omega_0 \left\{ \frac{\partial T^{ij}}{\partial\omega_0} \right\}_{\text{loc.eq.}}. \quad (16)$$

Considering small deviations from the local equilibrium, we may keep in (16) only first-order derivative quasiparticle terms  $\propto \partial_i$ , thus neglecting mean-field contributions  $\propto \partial_i \sigma \, \partial^j \sigma$  and  $\propto \partial_i \omega_0 \, \partial^j \omega_0$ .

The shear and bulk viscosities are as follows expressed through the variation of the energy-momentum tensor:

$$\delta T_{ij} = -\zeta \, \delta_{ij} \vec{\nabla} \cdot \vec{u} - \eta \, W_{ij}, \quad W_{kl} = \partial_k u_l + \partial_l u_k - \frac{2}{3} \delta_{kl} \partial_i u^i. \quad (17)$$

To find the shear viscosity, we put  $i \neq j$  in (17) and use that in this case the variation of the second and third terms in (16) yields zero after integration over angles. To find the bulk viscosity, we substitute  $i = j$  in (17) and use that  $T_{\text{eq}}^{ii} = 3P_{\text{eq}}$ . We put  $\vec{u} = 0$  in final expressions but retain gradients of the velocity.

Taking derivatives  $\partial F_a^{\text{loc.eq.}}/\partial x_a^\mu$  in Eq. (15) we find the variation of the total energy-momentum tensor as the function of derivatives of the velocity

$$\delta T^{ij} = \sum_a \int d\Gamma \frac{p_a^i p_a^j}{T E_a} \tau_a F_a^{\text{eq}} (1 \mp F_a^{\text{eq}}) q_a(\vec{p}; T, \mu_{\text{bar}}, \mu_{\text{str}}) \quad (18)$$

with

$$q_a(\vec{p}; T, \mu_{\text{bar}}, \mu_{\text{str}}) = \partial_k u_l \delta_{kl} Q_a - \frac{p_k p_l}{2E_a} W_{kl}, \quad (19)$$

$$\begin{aligned} Q_a = & - \left\{ \frac{\vec{p}_a^2}{3E_a} + \left( \frac{\partial P}{\partial n_{\text{bar}}} \right)_{\epsilon, n_{\text{str}}} \left[ \frac{\partial(E_a + X_a^0)}{\partial \mu_{\text{bar}}} - t_b^{\text{bar}} \right] \right. \\ & + \left( \frac{\partial P}{\partial n_{\text{str}}} \right)_{\epsilon, n_{\text{bar}}} \left[ \frac{\partial(E_a + X_a^0)}{\partial \mu_{\text{str}}} - t_a^{\text{str}} \right] - \left( \frac{\partial P}{\partial \epsilon} \right)_{n_{\text{bar}}, n_{\text{str}}} \times \\ & \left. \times \left[ E_a + X_a^0 - T \frac{\partial(E_a + X_a^0)}{\partial T} - \mu_{\text{bar}} \frac{\partial(E_a + X_a^0)}{\partial \mu_{\text{bar}}} - \mu_{\text{str}} \frac{\partial(E_a + X_a^0)}{\partial \mu_{\text{str}}} \right] \right\}. \end{aligned} \quad (20)$$

Finally, we obtain expressions for the shear viscosity

$$\eta = \frac{1}{15T} \sum_a \int d\Gamma \tau_a \frac{\vec{p}_a^4}{E_a^2} [F_a^{\text{eq}} (1 \mp F_a^{\text{eq}})], \quad (21)$$

and for the bulk viscosity

$$\zeta = -\frac{1}{3T} \sum_a \int d\Gamma \tau_a \frac{\vec{p}_a^2}{E_a} F_a^{\text{eq}} (1 \mp F_a^{\text{eq}}) Q_a. \quad (22)$$

At vanishing mean fields our results are reduced to those derived in Ref. [12].

## B. Collisional viscosity in baryon-less matter

In the relaxation time approximation both shear and bulk viscosities for a component "a" depend on its relaxation (collisional) time  $\tau_a$  which should be parameterized or calculated independently. Therefore to diminish this uncertainty it is legitimate at first to find the reduced kinetic coefficients (per unit relaxation time, assuming  $\tau = \text{const}$ , i.e.  $\tau = \tilde{\tau}$ ).

In Fig. 3 we demonstrate results of various calculations for the reduced shear (left panel) and bulk (right panel) viscosities scaled by the  $1/T^4$  factor at  $\mu_{\text{bar}} = 0$ . As we see from the figure, the reduced shear viscosity of the massive pion gas (dashed line) becomes approximately proportional to  $T^4$  for  $T \gtrsim 100$  MeV. Naturally, this result is close to that obtained in the Gavin approximation [19] (dashed-double-dotted line in Fig. 3). The  $T^4$  scaling is violated for the  $\pi - \rho$  gas in the temperature interval under consideration because the  $\rho$  mass is not negligible even at  $T \sim 200$  MeV. For  $\zeta$  the approximate  $1/T^4$  scaling property holds for the massive pion-rho gas at  $T \gtrsim 150$  MeV. Note that  $\zeta = 0$  for the gas of free massless pions since  $c_s^2 = 1/3$  in this case. For the massive pion gas  $\zeta/T^4$  decreases already for  $T > 60$  MeV reaching zero at large  $T$  similar to the massless gas. The reduced



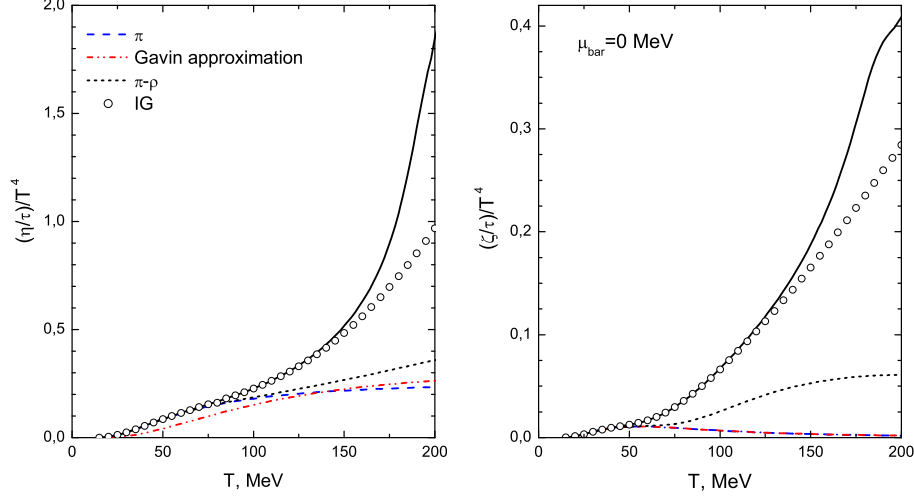


Рис. 3: The reduced (per unit relaxation time)  $T^4$  scaled shear (left panel) and bulk (right panel) viscosities as function of the temperature calculated within the SHMC model (solid lines) for the baryon-less matter,  $\mu_{\text{bar}} = 0$ . Results are compared with those for the massive pion gas (dashed lines),  $\pi - \rho$  mixture (short dashed lines) and with those for the massless pion gas (the Gavin approximation [19], dot-dashed line), as well as for the IG model (open dots) with the same set of species as in the SHMC model.

shear and bulk viscosities of a multicomponent system calculated in our SHMC model (solid lines) and in the IG model with the same hadron set (open dots) do not fulfill the  $T^4$  scaling law. These models include large set of hadrons, due to that with the temperature increase the reduced shear and bulk viscosities become significantly higher than those for the pion gas and the pion-rho gas models. An additional increase of the reduced viscosity within SHMC model originates from significant mass decrease at temperatures near the critical temperature. The bulk viscosity of a single-component pion system drops to zero both at low and high temperatures and in the whole temperature interval  $\zeta \ll \eta$ , that is frequently used as an argument for neglecting the bulk viscosity effects. However, the statement does not hold anymore for mixture of many species. For example, at  $T \sim 150$  MeV the  $\eta/\zeta$  ratio is only about 3 in case of the IG and SHMC models. Thus the bulk viscosity effects can play a role in the description of the hadronic stage at high collision energies, like at RHIC. Moreover, the bulk viscosity can be responsible for such important effect as flow anisotropy.

### C. Collisional viscosity in baryon enriched matter

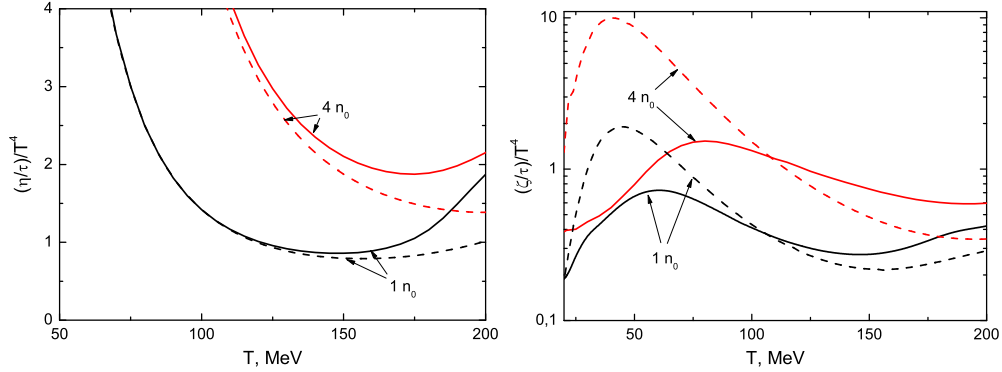


Рис. 4: The SHMC model predictions of the  $T^4$  scaled temperature dependence of the reduced shear (left panel) and bulk (right panel) viscosities calculated for hadron mixture at  $n_{\text{bar}} = n_0$  and  $4n_0$  (solid lines). Calculations performed in the IG based model with the same hadron set as in the SHMC model are demonstrated by dashed lines.

For the case of the multi-component hadron mixture within IG and SHMC models the temperature dependence of the reduced  $T^4$ -scaled shear and bulk viscosities are shown at baryon densities  $n_{\text{bar}} = n_0$  and  $4n_0$  ( $n_0$  is the nuclear saturation density) in the left and right panels of Fig. 4, respectively. The reduced shear viscosity calculated in the SHMC model (solid lines) is close to that in the IG model with the same hadron set (dashed lines). Differences in the  $\eta/(\tau T^4)$  ratio for the IG and SHMC models appear only at high temperatures  $T \gtrsim 150$  MeV. At  $T \lesssim 100$  MeV the reduced  $T^4$ -scaled bulk viscosity (right panel) in the IG based model proved to be larger than that in the SHMC model. Contrary, for larger  $T$  the reduced bulk viscosity in the IG model becomes smaller than that in the SHMC model. Differences come from the strong dependence of the bulk viscosity  $\zeta$  on the values of thermodynamical quantities (see Eqs.(20),(22)). Note that at  $T \gtrsim 100$  MeV and  $n_{\text{bar}} \gtrsim n_0$  the shear and bulk viscosities are getting comparable in magnitude. Growth of the relative importance of  $\zeta$  with increase of temperature seems to be quite natural because the bulk viscosity takes into account momentum dissipation due to inelastic channels which number increases with the temperature increase.

### D. Estimation of the relaxation time

The relaxation time is defined by Eq. (14). We implement free cross sections in case of the IG based model, similar to procedure performed in Ref. [20]. In case of the SHMC model, the in-medium modification of cross sections is incorporated by a shift of a “pole” of the collision energy by the mass difference  $m_a - m_a^*$  according to prescription of Ref. [21]. Due to a lack of microscopic calculations this is the only modification which we do here. Important peculiarity of the nucleon contribution to the relaxation time at low temperature is associated with the particular role played by the Pauli blocking. It means that appropriate multi-dimensional integration should be carried out quite accurately with using quantum statistical distribution functions. Calculations using the kinetic Uehling-Uhlenbeck equations for the purely nucleon system in the non-relativistic approximation were performed in [3]. For  $T \lesssim 100$  MeV an extrapolation expression has been obtained:

$$\tilde{\tau}_{NN} \simeq \frac{850}{T^2} \left( \frac{n_{\text{bar}}}{n_0} \right)^{1/3} \left[ 1 + 0.04T \frac{n_{\text{bar}}}{n_0} \right] + \frac{38}{T^{1/2}(1 + 160/T^2)} \frac{n_0}{n_{\text{bar}}} . \quad (23)$$

Thus the relaxation time demonstrates well known behavior  $T^{-2}$ , for  $T \rightarrow 0$ .

To simplify calculations we use Eq. (23) for the partial nucleon relaxation time  $\tilde{\tau}_{NN}$ , to be valid at low temperatures, smoothly matching it (at  $T \sim 100$  MeV) with the partial nucleon contribution calculated following Eq. (14) for higher temperatures. We take into account the whole hadron set involved into the SHMC model. The relaxation time for every component is evaluated according to Eq. (14).

### E. Collisional viscosity in heavy ion collisions

Above we have studied reduced viscosities of the hadron matter at different temperatures and baryon densities. In reality a hot and dense system being formed in a heavy-ion collision then expands towards freeze-out state, at which the components stop to interact with each other. Here we use the freeze-out curve  $T_{\text{fr}}(\mu_{\text{bar}}^{\text{fr}})$  extracted from analysis of experimental particle ratios in statistical model for many species at the given collision energy  $s_{NN}^{1/2}$  treating the freeze-out temperature  $T_{\text{fr}}$  and chemical potential  $\mu_{\text{bar}}^{\text{fr}}$  as free parameters [22, 23].

In Fig. 5, viscosity coefficients per entropy density  $s$  are shown versus the freeze-out temperature for Au + Au collisions (which is unambiguously related to the freeze-out

chemical potential  $\mu_{\text{bar}}^{\text{fr}}$  [22] needed to calculate thermodynamical quantities at the freeze-out). Dimensionless ratios of the viscosity to the entropy density  $\eta/s$  and  $\zeta/s$  characterize the energy dissipation in the medium. As we see, the  $\eta/s$  ratio decreases monotonously with increase of the temperature, being higher than the lower bound  $1/4\pi$  but tending to it with further increase of  $T_{\text{fr}}$ . The value  $\zeta/s$  exhibits a maximum at  $T_{\text{fr}} \sim 85$  MeV and then tends to zero with subsequent increase of  $T_{\text{fr}}$ . As has been emphasized above, at  $T \gtrsim 100$  MeV values of the shear and bulk viscosities become quite comparable,  $(\eta/s)_{\text{fr}} \simeq 2(\zeta/s)_{\text{fr}}$ .

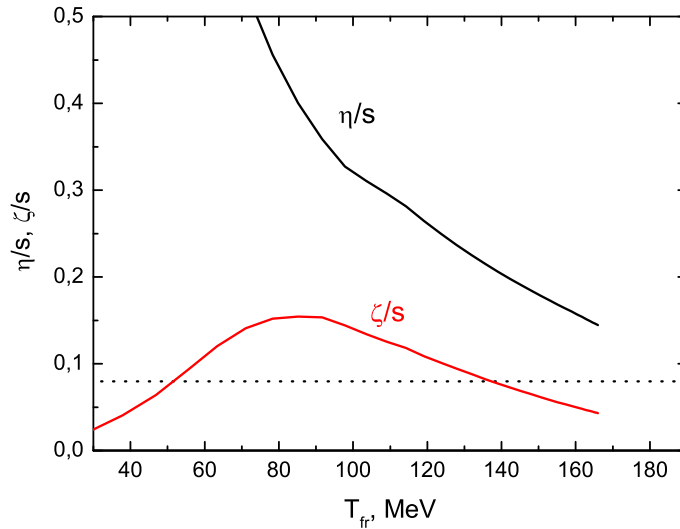


Рис. 5: Shear and bulk viscosities per entropy density calculated in the SHMC model for central Au+Au collisions along the freeze-out curve (at  $T = T_{\text{fr}}$ ) [22] for the baryon enriched system. The dotted line is the lower AdS/CFT bound  $\eta/s = 1/4\pi$  [11].

In Fig. 6, the  $\eta/s$  ratio calculated in our SHMC model (solid line) is plotted as a function of the collision energy  $\sqrt{s_{NN}}$  of two Au+Au nuclei. The result for the IG model with the same hadron set as in SHMC model is plotted by the dash-dotted line. We note that for  $\sqrt{s_{NN}} \gtrsim 3$  the SHMC results prove to be very close to the IG based model ones (with the same hadron set as in SHMC model), since the freeze-out density is rather small and the decrease of the hadron masses occurring in the SHMC model is not important. The results for the hadron hard core gas model (the van der Waals excluded volume model) [24] at two values of the particle hard core radius  $r$  are shown by dashed and short-dashed lines. In all cases for  $\sqrt{s_{NN}} \gtrsim 2$  GeV the ratio  $\eta/s$  decreases along the chemical freeze-out line with increasing the collision energy and then flattens at  $\sqrt{s_{NN}} \gtrsim 10$  GeV, since freeze-out at such high collision energies already occurs at almost constant value of  $T_{\text{fr}} \approx 165$  MeV. The shear viscosity of

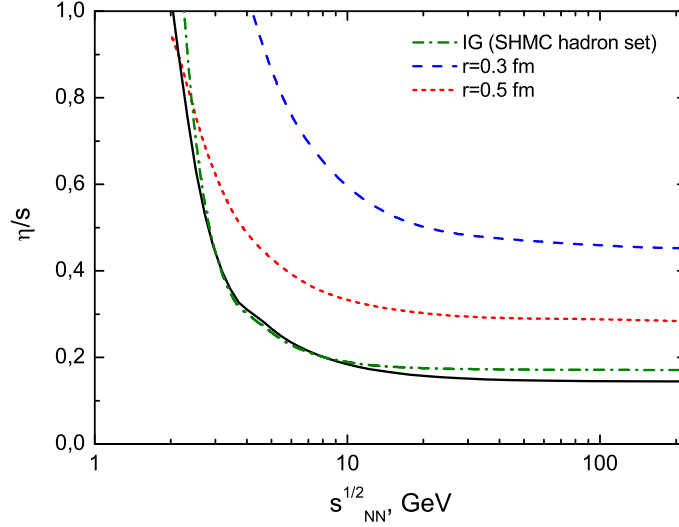


Рис. 6: The ratio of the shear viscosity to the entropy density calculated for central Au+Au collisions along the chemical freeze-out curve [22] within the SHMC model as a function of the collision energy  $s_{NN}^{1/2}$  (solid line). Dashed and short-dashed curves are the results of the excluded volume hadron gas model [24] with hard-core radii  $r = 0.3$  and  $r = 0.5$  fm, respectively. The dot-dashed line corresponds to the IG model with the same set of hadrons as for the SHMC model.

the non-relativistic Boltzmann gas of hard-core particles [24] is  $\propto \sqrt{mT}/r^2$ . Since Fermi statistical effects are not included within this model, the shear viscosity,  $\eta$ , decreases with decrease of  $T$ . Nevertheless the  $\eta/s$  ratio increases and diverges at low energy/temperature, as the consequence of a more sharp decrease of the entropy density compared to  $\eta$ , see Fig. 6. As follows from the figure, the smaller  $r$  is, the higher  $\eta/s$  is in the given excluded volume model. For  $\sqrt{s_{NN}} \gtrsim 4$  and  $r \simeq 0.7$  fm the  $\eta/s$  ratio is expected to be close to the values computed in the IG and SHMC models.

Recently an interesting attempt has been undertaken in [25] to extract the shear viscosity from the 3-fluid hydrodynamical analysis of the elliptic flow in the AGS-SPS energy range. An overestimation of experimental  $v_2$  values in this model was associated with dissipative effects occurring during the expansion and freeze-out stages of participant matter evolution. The resulting values of  $\eta/s$  vary in interval  $\eta/s \sim 1 - 2$  in the considered domain of  $\sqrt{s_{NN}} \approx 4 - 17$  GeV (corresponding to temperatures  $T \approx 100 - 115$  MeV) [25]. Authors consider their result as an upper bound on the  $\eta/s$  ratio in the given energy range. Note that mentioned values are much higher than those which follow from our estimations given above and presented in Figs. 5 and 6.

Other microscopic estimate of the shear viscosity to the entropy density ratio for the relativistic hadron gas based on the UrQMD code was performed in Ref. [26] where 55 baryon species and their antiparticles and 32 meson species were included. The full kinetic and chemical equilibrium is achieved at  $T = 130$  and  $160$  MeV, respectively. The extracted ratio  $\eta/s \gtrsim 1$  exceeds the SHMC result by a factor of 5. Introducing a non-unit fugacity or a finite baryon density allows one to decrease the ratio twice but nevertheless it is still too high as compared to both the SHMC result and the lower bound  $\eta/s = 1/4\pi$ . Analyzing their result authors [26] conclude that the dynamics of the evolution of a collision at RHIC is dominated by the deconfined phase (exhibiting very low values of  $\eta/s$ ) rather than by the hadron phase. Note however that in-medium effects in the hadron phase are not included into consideration in the UrQMD model though, namely, these effects result in the required decrease of the  $\eta/s$  ratio in our SHMC model.

#### IV. CONCLUSIONS

In this paper, we derived expressions for the shear and bulk viscosities in the relaxation-time approximation for a hadron system described by the quasiparticle relativistic mean-field theory with scaling of hadron masses and couplings (SHMC). The EoS of the SHMC model fairly well reproduces global properties of hot and dense hadron matter including the temperature region near  $T_c$  provided all coupling constants  $g_{\sigma b}$  are strongly suppressed except for nucleons. Thus obtained kinetic coefficients are compared with those calculated in other models of the hadron matter.

With increasing freeze-out temperature  $T_{\text{fr}}$  (for central Au+Au collisions), the  $\eta/s$  ratio undergoes a monotonous decrease approaching values close to the AdS/CFT bound at  $T \sim T_c$  MeV, while the  $\zeta/s$  ratio exhibits a maximum at  $T_{\text{fr}} \sim 85$  MeV. In a broad temperature interval the  $\eta/s$  and  $\zeta/s$  ratios are not small and viscous effects can be noticeable. The viscosity values at the freeze-out can be transformed into dependence on the colliding energy  $\sqrt{s_{NN}}$  (for central Au+Au collisions). When the collision energy decreases, the  $\eta/s$  goes up. The high-energy flattening of the  $\sqrt{s_{NN}}$  dependence occurs at quite low  $\eta/s < 0.2$ . It implies that a small value of  $\eta/s$  required for explaining a large elliptic flow observed at RHIC could be reached in the hadronic phase. This might be an important observation which we have demonstrated within the SHMC model.

The  $v_2$  analysis indicates to different values of  $\eta/s$  for peripheral and central collisions. Therefore, it would be interesting to perform hydrodynamic calculations using the  $T - \mu_{\text{bar}}$  dependent transport coefficients rather than constant ones. The need of such an approach was recently emphasized in [27]. Further we will use the SHMC model EoS with the derived transport coefficients for this purpose.

## Acknowledgements

We are grateful to K.K. Gudima, Y.B. Ivanov, Y.L. Kalinovsky and E.E. Kolomeitsev for numerous discussions and valuable remarks. This work was supported in part by the BMBF/WTZ project RUS 08/038, the RFFI grants 08-02-01003-a and 10-02-91333 HHIIO-a, the Ukrainian-RFFI grant № 09-02-90423-ukp-φ-a, the DFG grant WA 431/8-1 and the Heisenberg-Landau grant.

- 
- [1] J.L. Anderson and H.R. Witting, *Physica* **74** 466, 489 (1973).
  - [2] V.M. Galitsky, Yu.B. Ivanov and V.A. Khangulian, *Sov. J. Nucl. Phys.* **30** 401 (1979).
  - [3] P. Danielewicz, *Phys. Lett.* **B146**, 168 (1984); L. Shi and P. Danielewicz, *Phys. Rev.* **C68** 064604 (2003).
  - [4] R. Hakim and L. Mornas, *Phys. Rev.* **C47** 2846 (1993).
  - [5] J.I. Kapusta, arXiv:0809.3746[nucl-th].
  - [6] S.S. Adler et al. (PHENIX Collaboration), *Phys. Rev. Lett.* **91** 182301 (2003); J. Adams et al. (STAR Collaboration), *Phys. Rev. Lett.* **92** 052302 (2004).
  - [7] D. Teaney, *Phys. Rev.* **C68** 034913 (2005); P. Romatschke and U. Romatschke, *Phys. Rev. Lett.* **99** 172301 (2007); M. Luzum and P. Romatschke, *Phys. Rev.* **C78** 034915 (2008); K. Dusling and D. Teaney, *Phys. Rev.* **C77** 034905 (2008); H. Song and U.W. Heinz, *Phys. Lett.* **B658** 279 (2008); H. Song and U.W. Heinz, *Phys. Rev.* **C77** 064901 (2008); A.K. Chaudhuri, arXiv:0801.3180 [nucl-th].
  - [8] G. Policastro, D.T. Son and A.O. Starinets, *Phys. Rev. Lett.* **87** 081601 (2001).
  - [9] A. Peshier and W. Cassing, *Phys. Rev. Lett.* **94** 172301 (2005).
  - [10] E.V. Shuryak, *Nucl. Phys.* **A750** 64 (2005); M. Gyulassy and L. McLerran, *Nucl. Phys.* **A750** 30 (2005); U.W. Heinz, arXiv:nucl-th/0512051.

- [11] P. Kovtun, T.D. Son and O.A. Starinets, JHEP **0310**, 064 (2003); Phys. Rev. **94** 111601 (2005).
- [12] C. Sasaki and K. Redlich, Phys. Rev. **C79** 055207 (2009).
- [13] A.S. Khvorostukhin, V.D. Toneev and D.N. Voskresensky, Nucl. Phys. **A791** 180 (2007).
- [14] A.S. Khvorostukhin, V.D. Toneev and D.N. Voskresensky, Nucl. Phys. **A813** 313 (2008).
- [15] E.E. Kolomeitsev and D.N. Voskresensky, Nucl. Phys. **A759** 373 (2005).
- [16] F. Karsch, arXiv:hep-lat/0601013.
- [17] P. Castorina, J. Cleymans, D. E. Miller and H. Satz, arXiv:0906.2289 [hep-ph].
- [18] Yu.B. Ivanov, Nucl. Phys. **A474** 669 (1987).
- [19] S. Gavin, Nucl. Phys. **A435** 826 (1985).
- [20] M.Prakash, M. Prakash, R. Venugopalan and G. Welke, Phys. Repts., **227** 321 (1993).
- [21] E.L. Bratkovskaya and W. Cassing, Nucl. Phys. **A807** 214 (2008).
- [22] J. Cleymans, H. Oeschler and K. Redlich, Phys. Rev. **C73** 034905 (2006).
- [23] A. Andronic, P. Braun-Munzinger and J. Stachel, Nucl. Phys. **772** 167 (2006).
- [24] M.I. Gorenstein, M. Hauer and O.N. Moroz, Phys. Rev. **C77** 024911 (2008).
- [25] Yu.B. Ivanov, I.N. Mishustin, V.N. Russkikh and L.M. Satarov, arXiv:0907.4140 [nucl-th].
- [26] N. Demir and S.A. Bass, Phys. Rev. Lett. **102** 172302 (2009); arXiv:0907.4333 [nucl-th].
- [27] A. K. Chaudhuri, arXiv:0910.0979 [nucl-th].



## Аннотация

### **Вязкость адронной материи в релятивистской модели среднего поля со скейлингом адронных масс и констант связи**

А.С. Хворостухин, В.Д. Тонеев и Д.Н. Воскресенский

Сдвиговая ( $\eta$ ) и объемная ( $\zeta$ ) вязкости вычисляются в квазичастичном приближении времени релаксации для адронной материи, описываемой в рамках релятивистской среднеполевой модели со скейлингом адронных масс и констант связи. Представлено сравнение с результатами других моделей. Показано, что малое значение отношения сдвиговой вязкости к плотности энтропии, требуемое для объяснения большого эллиптического потока, наблюдаемого в экспериментах на RHIC, может быть достигнуто в адронной фазе. Отмечаются сравнительно большие значения объемной вязкости в случае барионо-обогащенной материи.